RIGHT WHALE LOCALISATION USING A DOWNHILL SIMPLEX INVERSION SCHEME

Francine Desharnais[1], Mathieu Côté[1], Colin J. Calnan[2], Gordon R. Ebbeson[1], David J. Thomson[1], Nicole E.B. Collison[1] and Chris A. Gillard[3]
[1]DRDC Atlantic, P.O. Box 1012, NS, Canada, B2Y 3Z7
[2]Xwave, 36 Solutions Dr, Halifax, NS, Canada, B3S 1N2
[3]DSTO, P.O. Box 1500, Salisbury SA 5108, Australia

ABSTRACT

The downhill simplex part of a hybrid nonlinear inversion procedure combining simulated annealing with a downhill simplex algorithm [S. E. Dosso and M.J. Wilmut, "An adaptive hybrid algorithm for geoacoustic inversion," Proceedings of the Fifth European Conference on Underwater Acoustics, 185-190 (2000)] was used to localize sounds from the workshop dataset. The procedure relies on relative arrival times for the direct propagation paths from the sources to each receiver. An eigenray model [S.E. Dosso, N.E.B. Collison, "Acoustic tracking of a freely drifting sonobuoy field," J. Acoust. Soc. Am. 111, 2166-2177 (2002)] was used to estimate travel time along the direct paths. The positions of the receivers and whales were obtained by inversion of estimated relative travel delays. It was found that the direct path assumption was a problem for the distances involved with the workshop dataset. This paper will discuss the solution of using a constant sound speed instead of actual sound speed profiles for localisation, as well as the error associated with arrival time inaccuracies. The error growth for multi-source cases will also be discussed.

RÉSUMÉ

Un algorithme de descente du simplexe faisant partie d'une procédure hybride d'inversion non linéaire combinant un recuit simulé et de descente du simplexe [S. E. Dosso et M.J. Wilmut, « An adaptive hybrid algorithm for geoacoustic inversion », Proceedings of the Fifth European Conference on Underwater Acoustics, 185-190 (2000)] a servi à localiser des sons dans un ensemble de données de travail. Cette procédure se fonde sur les temps relatifs d'arrivée pour des trajets de propagation directe entre les sources et chacun des récepteurs. Un modèle à vecteurs propres [S.E. Dosso, N.E.B. Collison, « Acoustic tracking of a freely drifting sonobuoy field », J. Acoust. Soc. Am. 111, 2166-2177 (2002)] a permis d'évaluer le temps de propagation sur des trajets directs. Les positions des récepteurs et des baleines ont été obtenues par l'inversion des délais de propagation relatifs estimés. Il s'est avéré que l'hypothèse des trajets directs posait un problème aux distances comprises dans l'ensemble de données de travail. Ce document examine la solution consistant à utiliser une vitesse de son constante plutôt que des profils réels de vitesse du son pour la localisation, ainsi que l'erreur liée aux imprécisions des temps d'arrivée. Le développement de l'erreur dans les cas de sources multiples est également abordé.

1. INTRODUCTION

In this paper, the downhill simplex part of a hybrid nonlinear inversion scheme that combines simulated annealing with a downhill simplex algorithm [1] is used to localise positions of North Atlantic right whales using a sparse array of five Ocean Bottom Hydrophones (OBHs). The sounds used were extracted from the DRDC/Dalhousie dataset provided at the *Workshop on Detection and Localization of Marine Mammals Using Passive Acoustics*, held at Dartmouth, NS, Canada, 19–21 November 2003.

A frequency-based cross-correlation procedure was used to determine relative arrival times of the right whale sounds on each OBH. Synthetic arrival times based on measured sound speed profiles were calculated using an eigenray model, assuming direct path propagation. The inversion procedure derived whale positions by minimizing the mismatch between the measured and modeled relative arrival times.

This paper describes the detection and localisation procedures, and presents the whale position estimate results. The effect associated with using a constant sound speed *vs.* an actual sound speed profile is discussed, as well as the

impact of detection times on localisation.

This paper concentrates on the 2002 workshop dataset. A 2000 calibration dataset was also available to the workshop participants. The 2000 dataset was also analyzed, and the results are included in Appendix A for reference. These results were also given to the workshop organizers to allow for comparisons with other authors.

Details regarding both datasets and a description of the experimental environment (Bay of Fundy) are given in an accompanying paper in these proceedings [2].

2. PROCEDURES

2.1 Arrival times

The detection algorithm used on the DRDC/Dalhousie dataset was kept simple on purpose. Although the accuracy of the technique is expected to be less than that associated with the cross-correlation techniques typically used in marine mammal localisation work [3,4], it was nonetheless adopted to introduce diversity in the comparison of results obtained with other techniques presented at the workshop. The use of a different detection scheme permits the effect of travel time error on localization accuracy to be assessed.

The technique utilized here consisted of first displaying a sonogram of the whale sound, as shown in Fig. 1. To produce this figure, a 1024-pt FFT was used with 90% overlap in time. A time and frequency window concentrating on the desired portion of the sound is selected from the gram (shown as the rectangle in Fig. 1). In the case of vocalizations, this selection was limited to one or possibly two of the strongest harmonics. In the case of a "gunshot" event, most of the frequency band was selected. For numerical convenience, the time window was adjusted to contain a multiple of the FFT size, centered on the pre-selected time period. This corresponds to approximately 0.85 s for the year 2002 dataset, where the sampling frequency was 1200 Hz. The time and frequency window selection was based on the sounds recorded on OBH sensor "L". The arrival times at mid-sound and the frequency band values are given in Section 3.1.

The sonograms of the signals recorded on all other OBHs were produced in a similar manner, and a first estimate of arrival time for the sounds were picked from these grams. A hanning window was then applied to the time series corresponding to the selected time window of each OBH. The windowed and filtered signal of OBH "L" was then cross-correlated in the frequency domain to the windowed signals of the other OBHs, following the technique of Carter and Ferrie [5], which is a different technique then [3,4]. The cross-correlation peaks defined the final relative arrival time delays of the sounds on all OBHs relative to OBH "L".

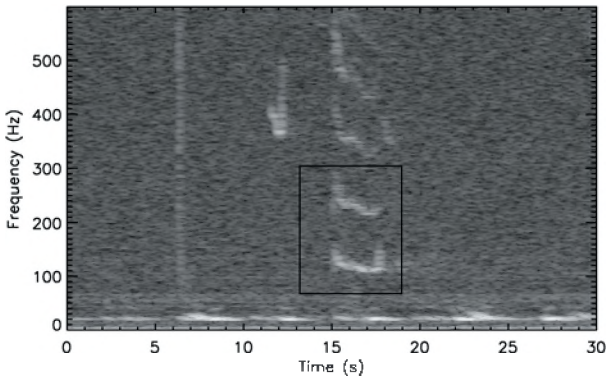

Figure 1. Sonogram of vocalization S131 as a function of time and frequency. The intensity levels are relative. The box represents the selected time and frequency band.

2.2 Localisation

Relative arrival times can be calculated from the measured sound speed profile with an eigenray model, and compared with the relative arrival times obtained from the cross-correlation techniques. Since the source position is unknown, an optimization technique is used to search the geographical space in an efficient manner. The estimated sound source position is taken as the location corresponding to the lowest error in the overall fit of the model to the data. The optimization algorithm is based on a hybrid nonlinear inversion procedure combining simulated annealing (SA) with a downhill simplex (DHS) algorithm. It should be noted that in the case of a simple geometric problem such as the inversion of one source and multiple receivers, the error surfaces are expected to present one clear minimum, and no secondary minima (except potentially in the vertical). For this reason, only the DHS part of the algorithm was used for this paper.

2.3 Eigenray model

The eigenray model described in Dosso and Collison [6] was used for this analysis. It provides expressions for the range r and arrival time t along a ray path between the source and receiver in an ocean with a sound speed profile $c(z)$, derived by applying Snell's Law to an infinite stack of infinitesimal layers. Both r and t are functions of $c(z)$ and the ray parameter $p = \cos(\theta(z))/c(z)$. In this model, the ray parameter for an eigenray connecting a source/receiver pair is determined by searching for the value of p that produces an r that equals the geometrical horizontal range (to a specified tolerance). Then this ray parameter is used to calculate the corresponding arrival time t.

2.4 Inversion engine

Inversion procedures have been used in the past for array element localization (AEL) problems, or to precisely localize elements of an acoustic array, using arrival times (if the source instants are known) or arrival time differences. For AEL, this problem has been solved either by linearizing the problem and using start up positions to iterate towards a final solution [7,8], or by searching the 3D space for solutions that will minimize the global relative arrival time error, with an algorithm such as simulated annealing [9].

The whale localization problem is similar to the AEL problem, though the receiving array in this case is very sparse, and the sources positions are completely unknown. In this paper, we chose to use an inversion procedure to search the 3D space for individual whale positions, while assuming the receiver positions to be known. The OBH receivers were located 0.9 m above the seabed and were known within 10 m in the XY plane. Changes in the receiver positions within this uncertainty resulted in negligible effects on the estimated source locations, and thus, fixed receiver positions could be used for the inversions. In this case, only the 3D position of the source was inverted for, using 4 relative arrival times, allowing the problem to remain over-determined.

The objective of the inversion algorithm is to search the model parameter space until a low mismatch value is found. The amount of mismatch between the model and data are calculated via a cost function. The cost function used here is the rms difference between the measured relative arrival times ΔT_{meas}, and the modelled relative arrival times ΔT_{model}:

$$E = \sqrt{\frac{\sum \left(\Delta T_{meas} - \Delta T_{model}(\mathbf{m})\right)^2}{N_{hyd} \cdot N_{src}}}, \qquad (2)$$

where N_{hyd} is the number of hydrophones, N_{src} is the number of sources, and the arrival times ΔT are relative to a reference hydrophone (OBH "L"). The model parameters $\mathbf{m}=[x_1,y_1,z_1,\ldots,x_M,y_M,z_M]$ are the 3D positions of the sources to be localized. The unit of the mismatch "E" is second [s].

The parameter space is searched with the DHS part of a hybrid Adaptive Simplex Simulated Annealing (ASSA) search technique developed by Dosso et al. [1,10]. ASSA combines the strengths of the downhill simplex method for minimizing a function locally and simulated annealing that is effective for global random search. Pure DHS minimization is based on an intuitive geometric scheme for moving downhill in a multi-dimensional space. The method operates on a simplex of M+1 models in an M-dimensional space. Each model is ranked according to its mismatch E and the simplex undergoes a series of reflections, expansions and contractions to work its way downhill. After each step, the difference between the highest and lowest mismatches relative to their average is used as a convergence criterion (10^{-5} was used in this paper). The primary advantages of the DHS method are that it retains a memory of regions where the function is small, and it is effective in navigating the search down the axes of long narrow parameter space valleys that are not aligned with the search parameter axes. These valleys are normally due to correlation between parameters in the search space. Whilst more efficient methods for finding local minima exist, the method is fast and efficient enough to use in the hybrid scheme of ASSA. The primary disadvantage of the DHS method alone is that it may become trapped in a local minimum and often must be started from many different points in the search space.

In this localization exercise, however, a single source is inverted for. The error surface for each source is expected to present a single minimum and no secondary minima (except potentially in the vertical, for particular deployment geometries other than ours) for known fixed receivers positions. In such a case, there is no risk of the DHS algorithm getting trapped in a secondary minimum, and is therefore used alone for the inversion.

3. RESULTS

3.1 Arrival times of the 2002 dataset

Table 1 summarizes the arrival times on OBH "L" (2002 dataset), as well as the frequency band selected for each whale sound for the cross-correlation. The arrival times on the other sensors (relative to OBH "L") are listed in Table 2. For reference, the results for the 2000 calibration dataset are listed in Appendix A.

Table 1. Arrival times on sensor "L" of selected sounds for dataset 2002, and processing bands used for cross-correlation.

Sound #	Sound name	Freq. band [Hz]	T_L [s]
1	S013-1	126-485	14.54
2	S035-2	29-550	15.31
3	S070-3	42-560	16.84
4	S093-4	40-534	14.71
5	S110-5	76-571	16.93
6	S092-7	79-222	16.07
7	S093-9	89-172	16.59
8	S131-10	58-157	13.02
9	S131-11	86-336	17.95
10	S131-12	68-274	17.01
11	S131-13	68-303	16.25
12	S134-6	71-448	17.44
13	S143-8	86-191	16.33
14	S209-14	308-542	15.31
15	S210-15	360-568	16.33

3.2 Localisation of the 2002 dataset

The 3D receiver positions were assumed to be known exactly, and were taken from [2]. The search space for the sources was limited by the bounds listed in Table 3. The bounds for the source positions were originally set to ±20 km for all sources; further analysis showed that two of the sources were located well south of the OBH pattern. The search space for these 2 sources was shifted south, but the 40 km ranges were preserved to simplify comparisons.

Table 2. OBH arrival times (ΔT's) for sensors "C", "E", "H" and "J" relative to sensor "L" for dataset 2002 (ΔT>0 denotes arrival on sensor "L" first).

Snd #	Snd name	ΔT_C [s]	ΔT_E [s]	ΔT_H [s]	ΔT_J [s]
1	S013-1	-0.92	1.45	6.58	5.61
2	S035-2	5.77	-1.88	-0.08	6.23
3	S070-3	-6.09	3.86	6.96	0.87
4	S093-4	6.09	5.22	-0.51	0.75
5	S110-5	-5.79	3.79	6.93	1.42
6	S092-7	5.85	5.25	-2.27	-0.83
7	S093-9	2.44	6.62	3.95	-4.59
8	S131-10	6.73	4.75	2.18	5.08
9	S131-11	7.27	4.62	2.25	5.17
10	S131-12	7.01	5.69	3.55	5.11
11	S131-13	7.04	5.65	3.49	5.12
12	S134-6	6.86	6.74	4.86	5.24
13	S143-8	0.96	4.79	6.99	4.26
14	S209-14	-3.37	-4.32	5.53	5.88
15	S210-15	-3.31	-4.36	5.20	5.82

Table 3. Search bounds used for the inversion. Values for the receivers are relative to individual OBH positions [2]; values for sources are relative to OBH "L", located at (0,0) in Cartesian coordinates.

	X	*Y*	*Z*
All sources but S209-14 and S210-15	±20 km	±20 km	0 to 214 m
S209-14 and S210-15	±20 km	-40 to 0 km	0 to 214 m

Each source position was inverted individually (one source per inversion event), using only the DHS part of the inversion algorithm. The sound speed profile that was measured closest in time to the sound recording time was selected for each individual sound [2]. For each inversion run, a new seed was used in the random number generator for an arbitrary initial search of the space, providing different final solutions for each run. Ten inversions were carried out for each source to provide a qualitative characterization of the algorithm variability, via a statistical distribution of the inversion solutions. On the order of 1000 to 2000 forward models were computed for each inversion.

The inversion algorithm converged for seven of the 2002 sources in this first attempt (sources #3, 8, 9, 10, 11, 12 and 13), based on the convergence criterion described in Section 2.4. The solution with the lowest mismatch *E* (for each individual source) is shown in Fig. 2. The origin of the plot is centered on OBH "L". The source numbers are as listed in Table 1. The mismatch *E* (or overall mismatch between the modelled and measured time arrivals) had an average of 0.128 s, excluding source #3 (S070-3), which had a mismatch of 3.54 s. The average inverted depth for the sources was 124 m. The inversion code did not converge for the remaining sources (sources #1, 2, 4, 5, 6, 7, 14 and 15).

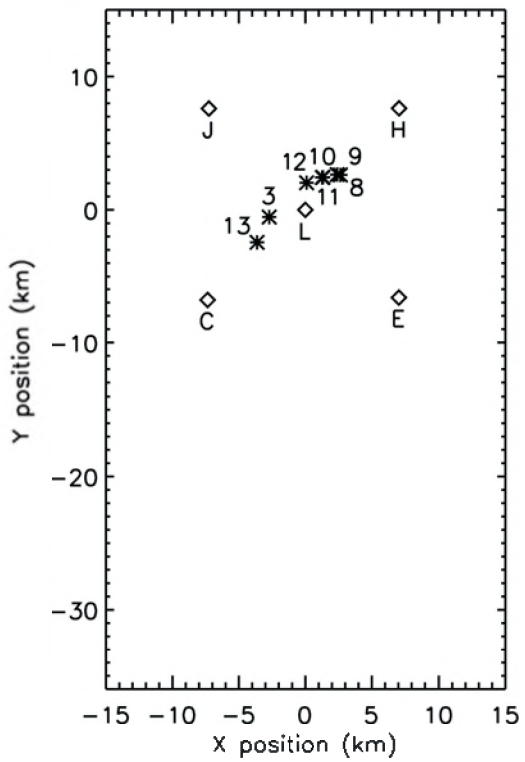

Figure 2. Localisation results using measured sound speed profiles. Diamonds represent OBHs; stars represents inverted sound positions. Sound numbers are as listed in Table 1.

In order to assess why the mismatch for source 3 was so large, and why some of the sources could not be localized, a ray plot was produced for a sound source located at 100-m depth. The left-hand side of Fig. 3 shows a simplified version of the sound speed profile from file "T7_00004.EDF", which was arbitrarily selected for this analysis; the right-hand side shows 20 rays traced at 2° intervals from 10° incidence below horizontal to 28° above horizontal.

It can be seen from Fig. 3 that a direct ray to the seabed

(where the hydrophones were located) does not exist for this source depth beyond approximately 6 km in range. If the source depth was shallower (results not shown here), the maximum propagation range would be shortened. For a source near the seabed, longer paths do exist, but refraction paths closer to the surface would lead to longer travel times.

The inversion code could not converge for sources that were located beyond the range of a direct path. For those sources where the algorithm did not converge, the average depth of 124 m corresponds to a compromise solution that minimized arrival time mismatch while allowing the rays to reach the sources.

3.3 The effect of constant sound speed

With an OBH pattern on the order of 14 km in extent, it is not surprising that direct paths cannot reach the required range in water depths of 220 m or less, unless the whales are near the middle of the pattern. As explained in [11], the multipath effect is aggravated by the position of the sensors near the seabed. The signals captured by the OBHs include multipath arrivals, and our cross-correlation technique has no way of distinguishing individual ray paths.

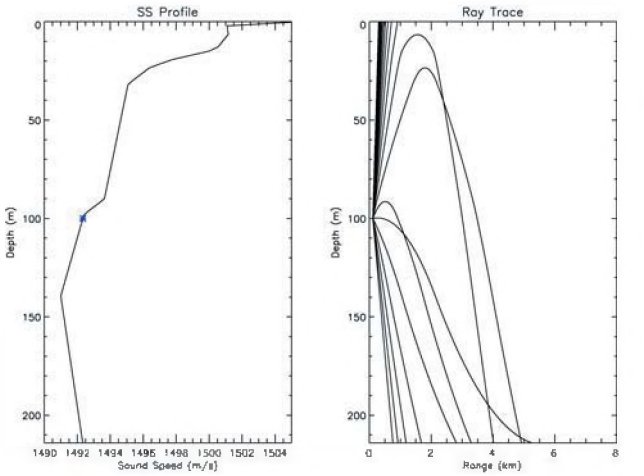

Figure 3. Sound speed profile (left panel) from "T7_00004.EDF" and ray paths (right panel) traced at 2° intervals from -10° to +28° grazing angle.

A simple method for avoiding this difficulty is to replace the measured sound speed profile with some average constant sound speed. In order to determine an effective constant sound speed, the behaviour of the mismatch E as a function of sound speed was investigated, using the sound that was arbitrarily selected from the first file (S013-1).

The sound speed was varied from 1488 m/s to 1502 m/s in increments of 1 m/s; a limit lower than the lowest sound speed in the water column was used as indirect paths treated as direct paths would imply a speed slower than the average sound speed in the water column. As before, the inversion procedure was carried out ten times for each sound speed, and the solution with the lowest mismatch E is plotted as a function of sound speed in Fig. 4.

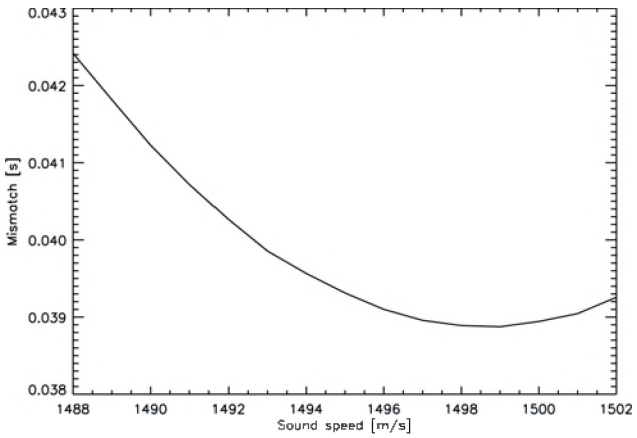

Figure 4. Mismatch *vs.* sound speed for sound S013-1.

The mismatch shows a broad minimum with a minimum value at a sound speed of 1499 m/s. This sound speed was therefore selected as an effective constant sound speed to use for each source. The inversion procedure was applied to each source using this effective constant sound speed, and the updated best results are shown in Fig. 5. Convergence was obtained for all fifteen sources.

These updated results show that several sources are now localized outside of the OBH pattern, as far as 35 km away from OBH "L", located in the middle of the pattern. The standard deviation of all ten runs was calculated as an indicator of the algorithm variability; it was on the order of 20 m inside the OBH pattern, and increased with range to reach 3 km for the two sources that are approximately 34 km south. This variability is a good indicator of the width of the minima in the mismatch surfaces for the various sources depending on their positions relative to the OBH pattern. The mean mismatch for all sources was 0.104 s, lower than the 0.128 s obtained with the actual sound speed profiles (Fig. 2). The source depths were again on the order of 120 m (from 80 to 152 m).

The difference between the results using the actual profiles (method A) and those obtained with a constant sound speed (method B) are summarized in Table 4, for the seven sources for which the algorithm converged. For these sources, the depth results were very similar for both methods, mainly within 17 m of each other. In the XY plane, the two methods localized sources within 15 m of each other, except for the third source (S070-3). The third

source had a very high mismatch when the actual sound speed profile was used (3.54 s), but it was reduced to 0.135 s with a constant speed of 1499 m/s. Fig. 5 also shows that the third source was localized outside of the OBH pattern by method B, over 11 km away from the position estimated by method A. It is believed that the new position is more accurate. Method A was able to converge on this source, but because of the direct path assumption, it could not reach the actual source location. The solution was not optimal, as demonstrated by the very high mismatch.

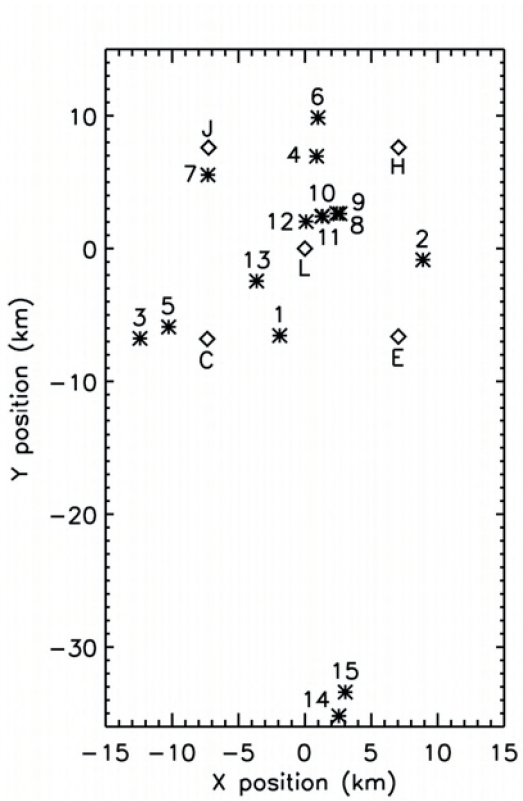

Figure 5. Localisation results using an effective constant sound speed of 1499 m/s. Diamonds represent OBHs; stars represents inverted sound positions.

Table 5 lists the best position estimates from method B. These final positions were used to compare the results of this localisation technique with those of other authors (see overall discussion on results elsewhere in these proceedings).

3.4 The impact of arrival times on localisation

As a further check on accuracy, the impact of arrival time estimates on inverted positions was investigated using arrival times from other authors. The cross-correlation scheme of Laurinolli *et al.* [12] was expected to lead to more accurate arrival times than the simple scheme used in this paper, as it takes full advantage of the time/frequency structure of whale vocalizations. Two of the sources with the smallest arrival time differences, and two of the sources with the greatest differences were selected for this test. The relative arrival times of Laurinolli *et al.* [12] were used to invert positions with the localisation technique described in Section 2.2. Table 6 shows the test results for these sounds. We emphasize that *E* {Laurinolli} in Table 6 indicates inversion results using the Laurinolli *et al.* arrival times, as opposed to their positions results.

Table 4. Differences between inverted positions using the actual sound speed profiles (method A) and an effective constant sound speed of 1499 m/s (method B), for the seven sounds for which both methods converged. $|\Delta XY|$ is the difference in horizontal distance. Values were rounded to the nearest integer.

Sound #	Sound name	$\|\Delta Z\|$ [m]	$\|\Delta XY\|$ [m]
3	S070-3	35	11528
8	S131-10	3	7
9	S131-11	8	7
10	S131-12	14	3
11	S131-13	11	0
12	S134-6	17	7
13	S143-8	5	13

Table 5. Best positions (lowest mismatch) with a constant sound speed of 1499 m/s. Values were rounded to the nearest integer.

Sound #	Sound name	*X* [m]	*Y* [m]	*Z* [m]
1	S013-1	-1899	-6551	126
2	S035-2	8884	-848	137
3	S070-3	-12417	-6768	111
4	S093-4	879	6950	77
5	S110-5	-10262	-5904	142
6	S092-7	987	9857	80
7	S093-9	-7305	5545	133
8	S131-10	2403	2642	115
9	S131-11	2639	2625	148
10	S131-12	1267	2425	117
11	S131-13	1335	2442	143
12	S134-6	91	2027	112
13	S143-8	-3639	-2446	135
14	S209-14	2558	-35192	152
15	S210-15	3037	-33394	86

Table 6. Comparison of results for selected sounds with the greatest and smallest differences in arrival times between Desharnais *et al* (this paper) and Laurinolli *et al.* [12]. Table includes general location of sound relative to OBH pattern, difference in detection times (averaged over all source/receiver pairs), difference in resulting positions (range and depth), and final energies.

	Greatest differences		Smallest differences	
Sound	S093-4	S134-6	S110-5	S210-15
Sound location	inside edge	middle	outside edge	30 km away
$\overline{\lvert\Delta T\rvert}$ [s]	0.24	0.19	0.04	0.06
ΔXY [m]	442	104	27	949
ΔZ [m]	-12	21	-4	16
E {Laurinolli} [s]	0.038	0.031	0.133	0.059
E {Desharnais} [s]	0.047	0.048	0.230	0.044

4. DISCUSSION

The downhill simplex part of a hybrid inversion technique combining simulated annealing with a downhill simplex algorithm was used to invert whale call positions using the sparse array of bottom-mounted sensors for the datasets provided for the *Workshop on Detection and Localization of Marine Mammals Using Passive Acoustics*, Dartmouth, NS, 19–21 November 2003.

Using the measured sound speed profile, it was found that several of the sources could not be localized because no direct path existed between the source and some of the receivers. All sources could be localized using an effective constant sound speed approximation.

It was found that low data/model mismatch values were obtained if the source positions were inverted individually using the downhill simplex part of the inversion algorithm only. Whether the full sound speed profile was used (*i.e.*, when a direct path existed between the source and all receivers), or a constant sound speed was assumed, the resulting 3D positions were usually within 15 m of one another. On one occasion, however, the constant sound speed approximation led to a change in estimated position in excess of 11 km. In this case, the high mismatch was a good indicator that the use of the actual sound speed profile led to a poor solution biased by the invalid assumption of an existing direct path.

The choice for an effective constant sound speed was based on a mismatch analysis for one of the sources. This may not have been the best choice for all of the sources, which occurred on different days and different locations. Future work will consider inverting for an optimized sound speed as well as optimized source and receiver positions.

The inverted source depth was usually on the order of 120 m, which is deeper than the presumed depth of vocalizing right whales [13]. With actual sound speed profiles, this depth was necessary to fulfill the requirement of a direct ray, since no direct ray exists at long range between a shallow source and a deep receiver. With a constant sound speed approximation, this depth optimized the data/model fit for the sound speed we selected. Either way, the depth estimates presented here are presumed to be inaccurate.

The issue of using a constant sound speed, or a direct path assumption was debated at length during the Workshop panel discussions. In this dataset, the direct path either does not exist, or is unlikely to be the arrival with the most energy, especially at long range. Our experimental arrival times are thus matched wrongly to direct path arrivals assumed by our eigenray model. The impact of this assumption is two-fold. First, the determination of relative arrival times will be affected, unless a full propagation model that includes multipaths is used. Second, the resulting XY position estimates can be biased. We believe that an optimization technique such as the one presented here, is likely to give good XY results if the source is located within a well-distributed array of receivers, since the biases on average should cancel out. If the source is located outside the receiver pattern, the errors will compound and grow with source-receiver range. The depth results will not be accurate in either case.

A simple frequency-based cross-correlation algorithm was used to determine relative arrival times. This technique does not take full advantage of the frequency/time structure of whale vocalizations. Yet, it led to consistent localization results within a 1 km diameter circle up to a range of 30 km from the positions based on arrival times determined from an alternative technique. For many purposes, this accuracy may be sufficient.

REFERENCES

[1] S. E. Dosso and M.J. Wilmut, "An adaptive hybrid algorithm for geoacoustic inversion," Proceedings of the Fifth European Conference on Underwater Acoustics, M.E. Zakharia, P. Chevret and P. Dubail, eds., Lyon, France, pp. 185-190, 2000.

[2] F. Desharnais, M.H. Laurinolli, D.J. Schillinger and A.E. Hay, "A description of the workshop datasets," Canadian Acoustics, June 2004.

[3] C. Clark and W. Ellison, "Calibration and comparison of the acoustic location methods used during the spring migration of the bowhead whale, Balaena mysticetus, off Pt. Barrow, Alaska," 1984-1993. J. Acoust. Soc. Am., 107(6), pp. 3509-3517, 2000.

[4] C. Clark, P. Marler, and K. Beeman, "Quantitative analysis of animal vocal phonology: an application to swamp sparrow song," Ethology, 76, 101–115, 1987.

[5] C.G. Carter & J.F. Ferrie, "A coherence and cross spectral estimation program," IEEE Programs for Digital Signal Processing, edited by the Digital Signal Processing Committee, IEEE Acoustics, Speech, and Signal Processing Society, pp. 2.3-1-18, 1979.

[6] S.E. Dosso, N.E.B. Collison, "Acoustic tracking of a freely drifting sonobuoy field," J. Acoust. Soc. Am. 111, 2166-2177 (2002).

[7] G.H. Brooke, S.J. Kilistoff, and B.J. Sotirin, "Array element localization algorithms for vertical line arrays," Proceedings of the 3rd European Conference on Underwater Acoustics, J.S. Papadakis, ed., Crete U.P., Heraklion, pp. 537-542, 1996.

[8] M. Barley, S. Dosso, and P. Schey, "Array element localization of a bottom moored hydrophone array, Canadian Acoustics 30(4), pp. 3-11, 2002.

[9] M.V. Greening, "Array element localization of rapidly deployed systems," Canadian Acoustics 28(2), pp. 7-13, 2000.

[10] S.E. Dosso, M.J. Wilmut, and A.S. Lapinski, "An adaptive-hybrid algorithm for geoacoustic inversion," IEEE J. Ocean Eng. 26, 324-336, 2001.

[11] D.M.F. Chapman, "You can't get there from here: shallow water sound propagation and whale localization," Canadian Acoustics, June 2004.

[12] M.H. Laurinolli, A.E. Hay, "Localisation of right whale sounds in the workshop Bay of Fundy dataset by sprectrogram cross-correlation and hyperbolic fixing," Canadian Acoustics, June 2004.

[13] Tyack, Pers. comm.

ACKNOWLEDGEMENTS

The authors would like to thank Dr. Stan Dosso (University of Victoria) for providing the initial ASSA code, and Marjo Laurinolli and her colleagues, for making their arrival time results available to us. This work was funded by Defence R&D Canada – Atlantic.

APPENDIX A. Results for the 2000 calibration dataset

A calibration dataset based on recordings from 2000 was made available to the participants. The results from the analysis of this dataset were given to the organizers to allow comparisons between authors and techniques. The results are presented here for future reference.

A1 Arrival times

Table A1 summarizes the arrival times determined for the 2000 dataset. For each whale sound, the frequency band selected for cross-correlation is also listed.

A2 Localisation of the calibration dataset

Our best position estimates for the 2000 calibration dataset are shown in Fig. A1 and Table A2. The positions were obtained with the measured sound speed profiles, not a constant sound speed. It should be noted that the transmissions may not have occurred at the RHIB boat positions, and therefore our positions should only be compared to other authors' positions, not to the known RHIB boat positions.

Table A1. OBH arrival times (ΔT's) relative to sensor "D" of selected sounds for dataset 2000 (ΔT>0 denotes arrival on sensor "D" first). Also shown is the processing band used for cross-correlation and the travel time to OBH "D".

Sound name	Freq. band [Hz]	T_D [s]	ΔT_B [s]	ΔT_C [s]	ΔT_E [s]
S282	300 – 570	4.69	-1.35	-1.49	-1.66
S282	300 – 570	3.35	-1.30	-1.42	-1.57
S288	50 – 250	3.20	-1.27	-1.50	-1.15
S289	50 – 250	3.10	-1.61	-1.90	-1.40

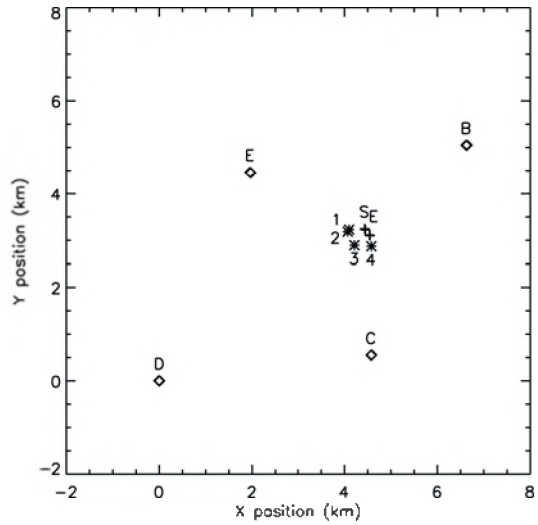

Figure A1. Positions of the sounds from the 2000 calibration dataset. "S" and "E" indicate the start and end positions of the RHIB boat where the playbacks were made from.

Table A2. Best positions (lowest mismatch) for the 2000 calibration dataset. Values were rounded to the nearest integer. Values are relative to OBH "D" located at (0,0).

Sound #	Sound name	X [m]	Y [m]	Z [m]
1	S282	4109	3229	119
2	S282	4107	3205	129
3	S288	4373	2903	103
4	S289	4619	2903	128